

Identification Of Multi-Class Skin Cancer Classification Using Relation Based Embedding Network With Few Shot Learning

Gopikha S¹ and Balamurugan M²

^{1,2}School of Computer Science and Engineering, Bharathidasan University, India.

Abstract

In order to have the best possible chance of survival for patients, early identification of skin malignancies such as melanoma is critical. Patient care could be improved through clinical use of Deep Learning-based Decision Support Systems for skin cancer screening. Many medical AI researchers focus on a diagnosis scenario that is primarily useful for autonomous operation. This is the primary emphasis of medical AI research. It is important, however, that practical decision support go beyond merely diagnosing and explain why. For dermatological disease diagnosis, the issue of clinical image classification is examined. Relation embedding networks are used to solve the challenge of few-shot classification, when a classifier has to generalise to classes that it has never seen before, with only a few examples of each novel class to work with few shot learning and classification can benefit from a relation-embedded network. Modules such as embedding metric mapping for feature vector evaluation and location detection for lesion identification during testing have been proposed in this work as two different modules. Using publicly obtainable skin lesion datasets, such as the SD-198 dataset, we evaluate the network's effectiveness and find that it outperforms than existing techniques with only a few annotated instances.

Keywords:- Skin Cancer; Relation-Embedding Networks; Image Classification; Few Shot Learning; Decision Support System.

Introduction

It's no secret that dermatological conditions are among the most common health issues of the modern era. Skin cancer [1,2] is one of the most lethal of these conditions. Uncontrolled cell growth is what cancer is all about [3]. As of today, skin cancer is frequently occurring malignancies in the globe [4, 5]. According to recent studies, the incidence of skin cancers, including melanoma and non-melanoma, has augmented meaningfully over the historical decade [5,6]. There are between 2 to 3 million skin cancers identified each year, as well as about 132,000 cases of melanoma [7]. The atmosphere's ability to absorb harmful sunlight is deteriorating on a daily basis, which is a major contributing factor [8]. Skin cancer cases are on the rise as a result of the thinned ozone layer [9].

Dermatologists to diagnose skin cancer, commonly use Dermoscopic pictures, as well as biopsy and histological investigation. But these procedures are time-consuming and highly sensitive to human mistake. Early discovery and treatment of skin cancer have been shown in numerous studies. As a result, it is critical to be able to quickly and accurately classify dermoscopic images. In today's world, AI technology can pre-diagnose a wide range of illnesses.

For example, driverless vehicles, search engines, art creation, and medical diagnostics are all examples of AI uses. Promising results were reached in the case of ML detection by using AI, and the sole reliable solution is no longer only optical inspection of skin lesions. Classical ML algorithms, a subset of AI, were first offered as a solution for automatic detection of anomalies. It is through the utilisation of earlier results that ML mostly enhances the current ones [10]. Firstly, the system pulls the features it needs to build training data from its database. Unsupervised or supervised learning is employed in the learning process after training data has been gathered. The supervised learning models, which are more accurate, were utilised in the majority of studies. Traditional machine learning approaches have shown promising outcomes but also certain drawbacks in other areas where they have been used. It takes time to train the system, requires a big amount of data to do so, and has a high rate of error-susceptibility. In response, the authors turned to NN and DL methods.

It's been suggested in the literature that there are several methods for dealing with scarce data, including transfer learning [11-12] and few-shot learning [13], both of which call for the network to be trained on a huge sum of labelled data from a connected domain before being fine-tuned on data from the target field. When it comes to medical images, meta-learning approaches have been successful in classifying real-world image datasets [14-16]. One area of medicine where meta-learning approaches have not been thoroughly studied by researchers is the classification of skin lesions. There is a limited sum of examples available for a significant number of current or emerging skin disorders, which necessitates the application of meta-learning approaches in the classification of skin lesions. Prototypes for each illness class were learned using clustering and an online updating approach, according to Prabhu et al. [17]. Other researchers [18] devised a difficulty-sensitive approach to meta-learning that dynamically checks the relevance of learning tasks throughout meta-optimization, which they tested their network on ISIC 2018 skin lesions.

Two separate modules are utilised in this study to pinpoint the exact location of the skin cancer. In the beginning, the Max-norm CNN is used to extract the features of skin cancer, which is used to classify the skin cancer images. If the skin cancer is malignant that a few-shot learning process is carried out to identify the sub-type of melanoma involved. Only acral lentiginous melanoma and lentigo maligna are considered in this study. Detailed explanations of the sub-sections are provided in the following paragraphs.

2. Related Works

By combining hand-crafted features with automated features retrieved from deep CNN models, Filali et al. [19] suggested a skin lesion categorization technique. PH2 and the ISIC

challenge datasets were used to train and assess the model. The PH2 dataset performed better in the experiments, as evidenced by the results.

Deep feature fusion was proposed by Amin et al. [20] as a means of detecting skin cancer. AlexNet and VGG-16 are used to extract relevant features from the segmented skin lesion images, which are then combined for use in the classification challenge. PCA was used to find the best possible mixture of features. The model was trained and validated using a carefully chosen dataset.

Deep neural networks were used by Bajwa et al. [21] to improve classification performance while classifying hundreds of skin disorders. DermNet and ISIC are two of the most widely used datasets for identifying skin lesions, and the researchers were able to reach 80% and 93% accuracy, correspondingly. Bi et al. [22] also obtainable a hyper-CNN classical for multi-modal skin lesion categorization. When the distribution of classes is imbalanced [22], their method can produce reliable classification results.

A strategy for early detection of melanoma was presented by Xu et al. [23]. Feature extraction, image segmentation, image noise reduction, and classification were all done sequentially. An improved CNN employing the satin bowerbird optimization (SBO) was used for segmentation in the study. SBO was used to focus on only the most significant details in the segmented images before they were further processed. Last but not least, the photos were classified using SVM, a support vector machine. The procedure was tested against the database of the American Cancer Society, and the findings revealed that it was effective. Due to a mix of deep learning and SBO algorithm, the method generated a complex system, but the results were good.

According to Dey and colleagues [24], an ideal machine vision technique for melanoma diagnosis has been developed. Diagnoses were made more accurate due to the usage of the Bat algorithm. Distance-regularized level-set (DRLS) was used to segment the melanoma. Accordingly, the PH2 database was analysed to demonstrate the method's correctness by analysing significant image performance metrics (IPM).

3. Motivation and Objective of the Model

To us, human intelligence's ability to learn from a limited sum of samples and its capacity for utilising existing knowledge and experience to solve new challenges motivates us. It's quite difficult to have access to vast amounts of medically-labeled data while dealing with skin cancer disorders. A cancer diagnosis necessitates extensive data collecting, which may be both time-consuming and expensive. As a result, a support system for medical specialists is needed to speed up and recover the accuracy of essential disease diagnosis. This problem has been addressed in part through the development of deep learning and machine learning simulations. In order to accurately categorise a given collection of test photos, deep learning procedures require a massive sum of data. In multi-skin cancer cases, this is usually not an option. Generalization capacity can be adversely affected and the model may be highly biased by training on a small sum of examples. As a result, new approaches are needed to address the issue of data scarcity. There are a number of ways in which meta-learning can be applied, particularly in the medical field. This is why we have presented a meta-learning strategy that

works with a small number of data samples to overcome all of these obstacles and improve the generalizability of the classification model for skin cancer disorders.

From skin lesion photos, researchers hope to diagnose illnesses. The distribution of images for various types of skin lesions is frequently skewed in picture databases. As new and unusual diseases are discovered daily, it is becoming increasingly difficult to annotate them due to a lack of knowledge. If you have a disease that is novel or rare, you may not have enough annotated samples. Using standard deep networks to categorise skewed skin lesion datasets does not generalise well because they acquire biased class priors toward the classes with more samples and perform poorly on rare disease classes. In addition, training deep networks repeatedly is a time-consuming procedure, which is typically undesirable in healthcare. As a result, new approaches of learning and adapting to new disease classes are being sought for. As a result, we define the challenge of disease detection from skin lesion photos in low-data regimes as a few-shot learning problem using contemporary meta-learning approaches. Relation-embedding networks are the name given to our suggested approach for discovering novel or atypical sickness classes with a limited amount of annotated data. As part of the meta-training learner's of the neural network, it uses a large sum of few-shot picture classification problems to determine effective network for the model and to train the neural network.. An embedding metric mapping module is part of the meta-learning technique. The model is then tweaked in the meta-testing stage so that it can classify previously unknown or rare classes with a dwindling number of examples. YoloV5 network is used for location detection module and ISIC 2018 dataset is used for training process and SD-198 dataset is used for testing process. At first, the proposed model is used to identify the skin cancer as melanoma or benign. Finally, the proposed model label the two different types of skin cancers such as Acral lentiginous melanoma and Lentigo maligna.

3. Proposed System

3.1. Dataset description

There are 10,015 dermoscopic images in the ISIC 2018 Skin Lesion dataset [25] that are utilised as a task sampler which contains support set and query set. Various dermatoscopes and anatomical locations were used to collect the data. According to the dataset's distribution of disorders, benign lesion photos are better represented than malignant lesion images. The photos have a height and width of 600 pixels each. This is the most common location for a target lesion. Six class diseases of malignant and benign lesions, such as melanoma, basal cell carcinoma, actinic keratosis, dermatofibroma, vascular lesion, and Squamous cell carcinoma, can be treated in dissimilar ways and for different lengths of time, so it is important for the physician to be able to distinguish between the two in order to establish an accurate diagnosis. Lesions, with the exception of vascular lesions, all of which have forms that are completely devoid of pigmentation, exist (for example amelanotic melanoma). As part of our proposed work, we used both the 6-way-3-shot approach and the 6-way-5-shot method by considering these six skin cancer diseases. It's shown in Figure 1: a selection of photos from this dataset.

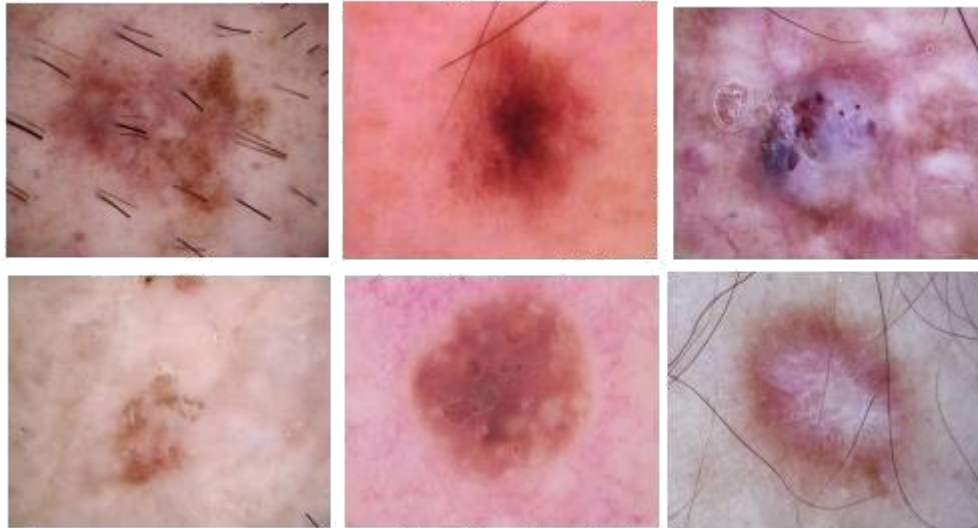


Figure 1: Sample images

Skin disease categories from eczema, acne and malignant illnesses are included in the SD-198 [26] dataset, which has 198 fine-grained disease classifications. In total, there are 6,584 photos. A wide variety of patients of all ages, genders, areas of disease, colours of skin, and different phases of the disease are depicted in the photographs. SD-198 provides a 3,292 training and 3,292 testing images, which is annotated by Yolo-V5 network's bounding box. Digital cameras and cell phones are used to capture the photographs. Resized from 1640 x 1130 to 224 x 224 pixels, the original image size. For testing, we utilise a two-way-3-shot approach, and we use a two-way-5-shot method. Figure 2 depicts the results of the two-way, three-shot approach used to detect acral lentiginous melanoma.



Figure 2: Sample images for acral melanoma.

An uncommon form of skin cancer that develops on the palms, soles, or under the nails of the fingers or toes is known as acral lentiginous melanoma. It is the most recurrent kind of melanoma in those with darker skin. Figure 3 depicts the results of the 2-way-5-shot approach in action on a lentigo melanoma.



Figure 3: Sample images for lentigo melanoma.

When melanocytes are only found in the epidermis of the affected area, it is referred to as "in situ" melanoma because of its rarity among early melanoma forms. It's most common on sun-damaged skin, so you'll see it most often on the nose and cheeks. There is a gradual increase in size over a period of 5 to 20 years or more.

3.2. Problem Definition for Meta-Learning Purpose

Let $\mathcal{D} = \{ \mathcal{D}_1, \mathcal{D}_2, \dots, \mathcal{D}_n \}$ signifies total of n datasets (here two skin cancer dataset images are used) and each dataset is defined as $\mathcal{D}_i = \{ (x_i, y_i) \}_{i=1}^n$, where (x_i, y_i) match an image with its corresponding description. Each dataset is divided into two sets: a meta-test set ($\mathcal{D}_{\text{meta-test}}$) that includes photos from classes with fewer representative images (rare diseases), and a meta-train set ($\mathcal{D}_{\text{meta-train}}$) that includes images from classes with more representative images. ($\mathcal{D}_{\text{meta-train}}$) is an important concept here, and it is used to learn initial weights and fine-tune on challenges where data is scarce. Our goal is to train a neural network model $\theta = (\theta; \omega)$ to perform well on short-term tasks taken from the $\mathcal{D}_{\text{meta-test}}$ data set to simulate the problem of data scarcity. To generalise successfully, deep learning algorithms necessitate enormous volumes of data that are dispersed over many classes. However, when faced with a few-shot learning challenge, they fall short of expectations in terms of accuracy. As a result, our approach makes use of the meta-train set to discover stronger initial weights, which are subsequently fine-tuned on new datasets.

3.3. Few-shot meta learning

" n " specifies the sum of images per class that can be used for learning in k -way, n -shot learning problems like this. This is an example of a circumstance in which the model is shown 10 photos, five of which are from each category. The meta-training and meta-update stages are included in each episode of the meta-learning paradigm. A series of incidents characterises the learning process. $\theta = (\theta; \omega)$, where x is the input and the θ is weights of the neural network, is the base learner model. The meta-parameter sets the classification perfect $\theta = (\theta; \omega)$ to the initial value of θ for each of the k tasks in a collection of m such tasks. Meta parameters are updated using task parameters, and the update rule is:

$$\theta' \leftarrow \theta + \frac{1}{m} \sum_{i=1}^m (\theta_i - \theta) \quad (1)$$

A total of n_k photos will be used for fine-tuning the weights for each n -way k -shot job sampled from D (meta-test). Then, ' n ' photos are used to measure the model's accuracy on the test ($D_{\text{(meta-test)}}$). Cross entropy loss was utilised to update the model's weights during meta-training and meta-testing. The cross entropy loss for a given task T_i is mathematically denoted by the expression

$$L_i = -\sum_{c \in \mathcal{C}_i} p_c \log(p_c) + (1 - p_c) \log(1 - p_c) \quad (2)$$

Where (x, y) is the input and label pair.

3.4. Proposed Meta-Learning/Meta-Training

In meta-training, the ISIC 2018 dataset has been used. In the support set, the image label pairs are presented, where the task samples are developed by using the following Eq. (3):

$$L_i = \frac{1}{|\{(x, y) \mid x \in \mathcal{X}_i, y \in \mathcal{Y}_i\}|} \quad (3)$$

Where, \mathcal{X}_i is denoted the set of unseen X classes in the support set and \mathcal{Y}_i is denoted the set of unseen Y classes in the support set. This support set with unseen classes and seen classes has no intersection, which is defined in Eq. (4):

$$\mathcal{X}_i \cap \mathcal{Y}_i = \emptyset \quad (4)$$

Where, base dataset seen classes is denoted as \mathcal{S} and support set unseen classes is denoted

as \mathcal{U} . To learn a classifier in few shot learning (FSL), $\mathcal{S} \rightarrow \mathcal{U}$, where Image's feature (f) to be recognized at test time. It comes only from the unseen classes (\mathcal{U}). In meta testing, each task sampler will create the meta task with support set and query set.

In this research work, seen classes is taken from ISIC 2018 dataset and unseen classes is taken from SD-198 dataset.

Each image from query set (\mathcal{Q}) and support set (\mathcal{S}) images has fed into max norm CNN model, the model extracts the feature vector /embedding and embedding module collects the feature vector, the embedding metric mapping module evaluate cosine similarity and cosine distance between feature vector to the support set embeddings. Cosine similarity i.e. $(f, s)_{s \in \mathcal{S}}$ is evaluated between the feature vectors. The cosine distance is calculated by using the following Eq. (5):

$$1 - (f, s)_{s \in \mathcal{S}} = (f, s)_{s \in \mathcal{U}} \quad (5)$$

The unseen query set classifier is defined by \rightarrow (). If the cosine similarity is high and cosine distance is less then metric score will be high. If the cosine similarity is low, and cosine distance is high then metric score will be low. Based on the metric score, label classification is done. The cross entropy Loss on the resulting classification is backpropagated through the CNN model. Algorithm 1 is used to explain the whole process and Table 1 shows the notation description, which is used in the algorithm.

<p>Algorithm 1: Workflow of proposed model</p> <p>Input: Query set of unseen classes and Support Set ,</p> <p>Output: ().</p> <p>for = {(, ,)} , =1</p> <p> return ,</p> <p>Calculate (,)</p> <p>Evaluate(,) = 1 - (,)</p> <p>Return()</p> <p>().</p>

Table 1: Notation Description

Notation	Description
	Query set of unseen classes
,	Support set of unseen classes
,	Feature Vector
	Cosine Similarity by between vectors
()	Cosine Distance
()	Metric Score
().	Classification of new unseen classes.

3.5. Proposed Meta-Testing

In Meta testing, SD -198 dataset has been used. This includes the concept of two step verification.

Step 1:

The dermatologists are able to verify their position with the help of the location detection module during testing. The YoloV5 [27] network is used in this study to perform the location detection module operation. For example, the location of diseases like acral and skin cancer is provided to the query set, which includes specific diseases like these. Using the YoloV5 network's position detection module, we were able to identify the location of the lesion in each query image by defining a bounding box around it. SD-198 has been annotated and the lesion's exact location/spot has been discovered using this yolov5 network.

Step 2:

The same image from query set and support set images has fed into max norm cnn model. It consists of 15 layers composed of four sets of consecutive layerwise maxnorm conv2D constraint layers, max pooling followed by global average pooling, flattening, Maxnorm

Dense layer and finally the classification layer. The patched uprooted skin lesion dataset is used for training and testing. The patch uprooted RGB image is fed as an input with a size of (224,224,3) to the proposed model. For each maxnorm weight constraint layer, the vector norm of the incoming weight at each hidden unit is bound to a limit m . The magnitude of the vector is calculated using maxnorm. By customising the weights in each max norm conv2d layer, kernel constraints and bias constraints values are fixed. This has the effect of limiting the weight matrix as a whole immediately. Weights with a maxNorm greater than m should be scaled down to that norm by a factor that is equal to m .

Finally, the model extracts the feature vector /embedding and embedding module collects the feature vector. The embedding metric mapping module evaluate cosine similarity and cosine distance, which is already defined in the meta-learning phase. If the cosine resemblance is high and cosine distance is less then metric score will be high. If the cosine similarity is low, and cosine distance is high then metric score will be low. Based on the metric score, label classification is done. Each query image is classified by evaluating the cosine resemblance and cosine distance between feature vectors to the support set embedding. Figure 4 shows the working flow of proposed methodology.

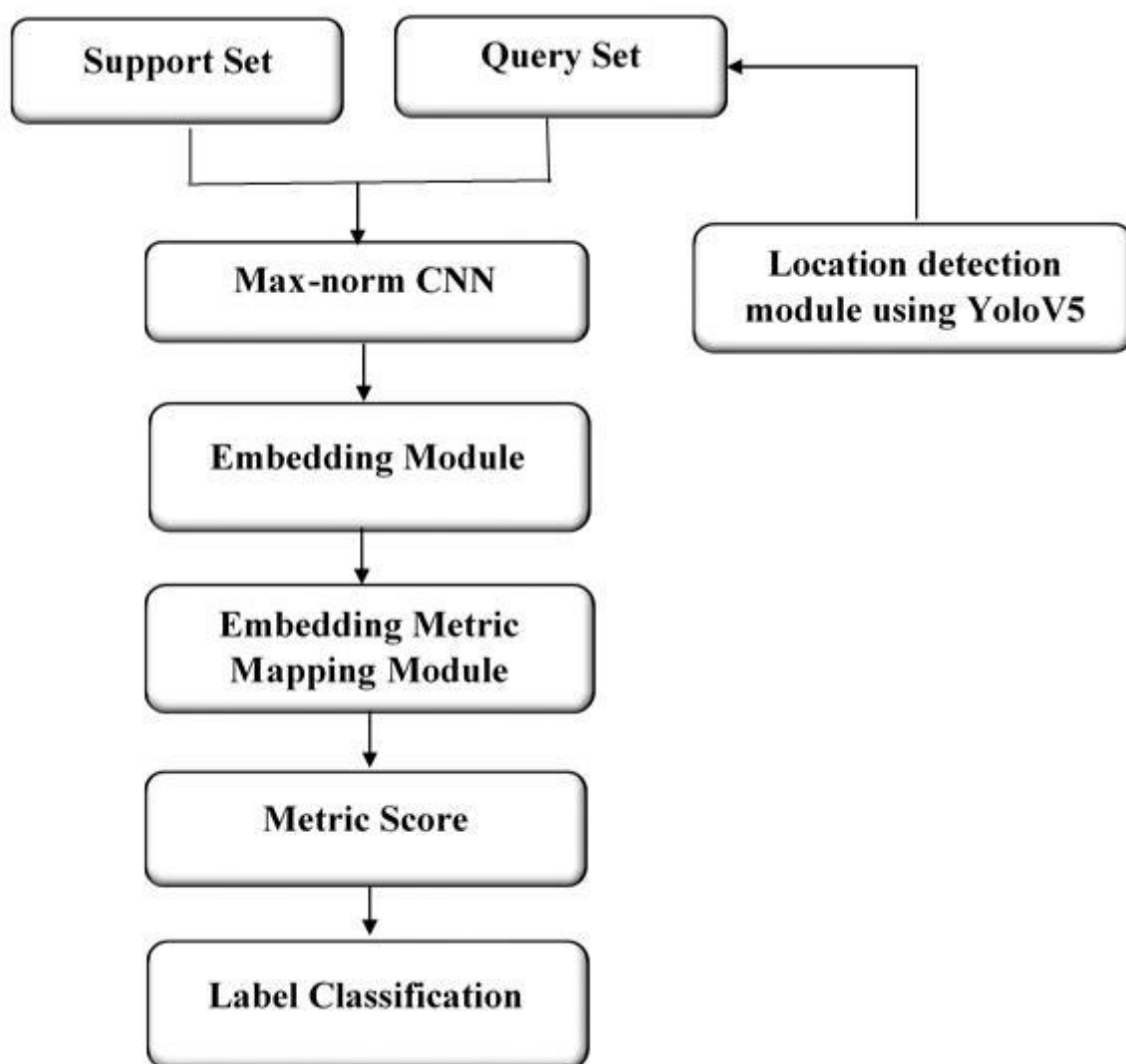


Figure 4: Overall Working Flow Diagram

4. Results and Discussion

There were 64GB of Dual Channel RAM used to train the networks. Tensorflow GPU 2.4.1 and Keras 2.3.1 were used in the software configuration on Windows 10. In this research work, average accuracy and average AUC are used for validation. The proposed model is tested with two datasets, where Table 2 and graphical representation in Figure 5 and 6 shows the performance for ISIC 2018 dataset in terms of AUC and accuracy.

Table 2: Performance Analysis of projected model with existing techniques on ISIC dataset for classification of 2-way

No. of Few shot learning	G-Conv [28]		Meta Med [29]		Proposed Relation-embedding network	
	Avg. AUC	Avg. Accuracy	Avg. AUC	Avg. Accuracy	Avg. AUC	Avg. Accuracy
3-shot	69.01	71.20	76.87	72.16	80.40	75.14
5-shot	74.16	79.14	79.01	80.19	85.70	83.10

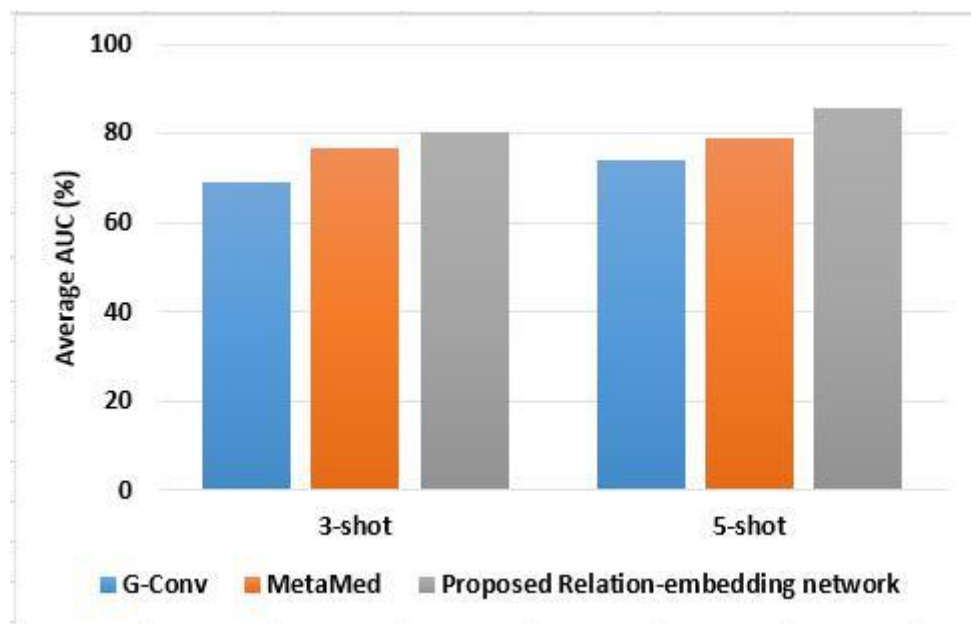


Figure 5: Graphical Depiction of projected model on ISIC-2018 dataset in terms of AUC.

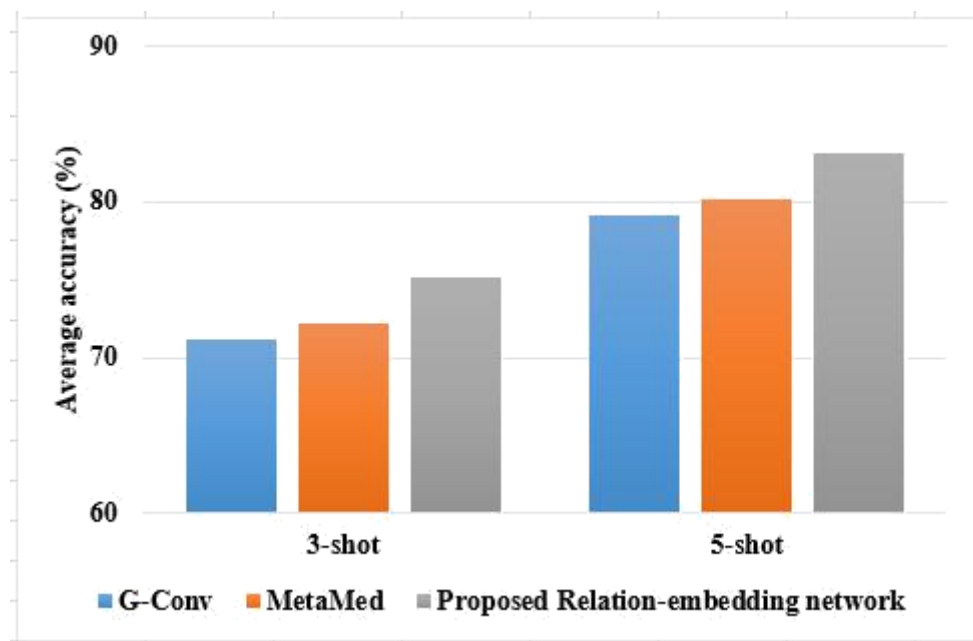


Figure 6: Graphical Illustration of projected model on ISIC-2018 dataset in terms of Accuracy

The support set will only provide additional information at the test time. While performing few shot learning, prediction accuracy depends on the number of ways and number of shots. As the number of shot increases, the prediction accuracy also improves. In the 5-shot learning, the proposed model achieved 85.70% of AUC and 83.10% of accuracy, where the existing techniques achieved nearly 79% to 80% of AUC and accuracy. The reason for better performance of proposed model is that it classifies initially whether the skin cancer is benign or malignant, where other models directly performs on all skin cancer images, which leads to poor classification accuracy. The experiments on second dataset is shown in Table 3 and graphical representation is given in Figures 7 and 8.

Table 3: Performance Analysis of proposed model with existing techniques on SD-198 dataset for 2-way classification

No. of Few shot learning	G-Conv [27]		Meta Med [28]		Proposed Relation-embedding network	
	Avg. AUC	Avg. Accuracy	Avg. AUC	Avg. Accuracy	Avg. AUC	Avg. Accuracy
3-shot	79.25	76.53	80.17	79.43	83.34	84.61
5-shot	80.41	84.67	83.13	87.92	89.60	91.28

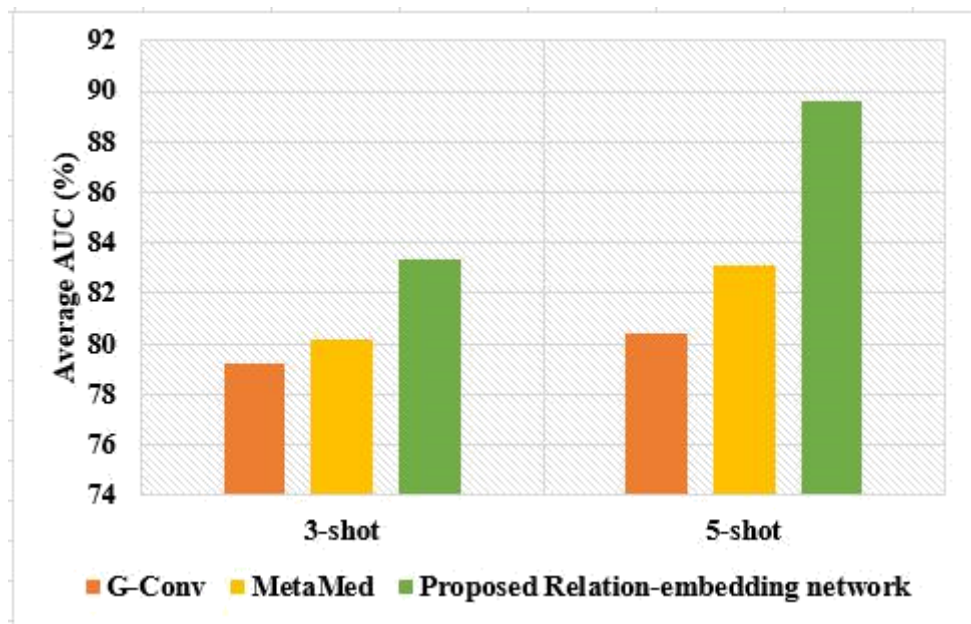


Figure 7: Graphical Representation of proposed model on SD-198 dataset in terms of AUC

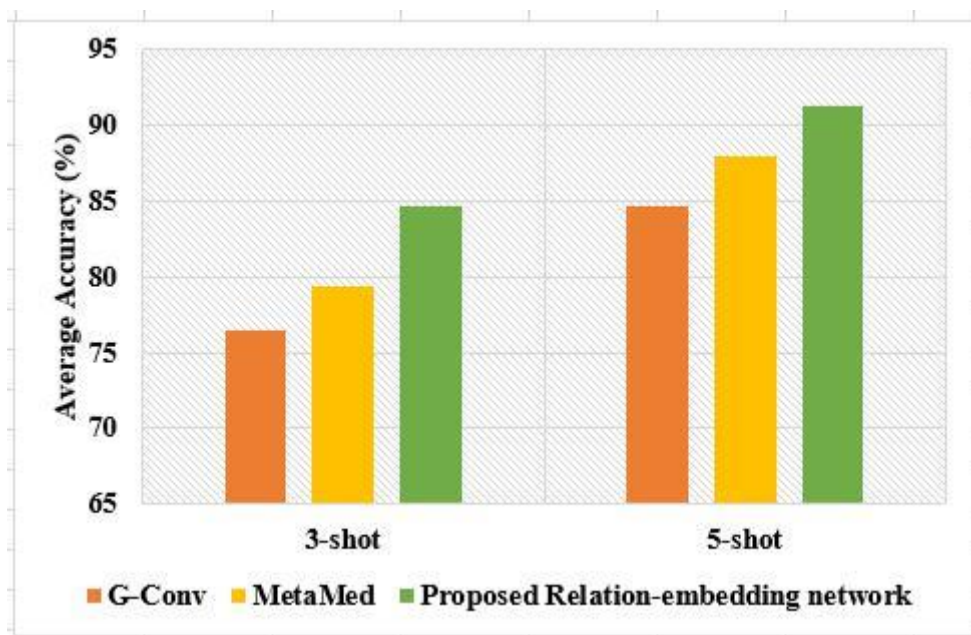


Figure 8: Graphical Representation of proposed model on SD-198 dataset in terms of Accuracy

When the few shot learning is less, the performance is also less for all techniques. For instance, the G-Conv model achieved 79.25% of AUC and 76.53% of accuracy on 3-shot learning and also the same model achieved 80.41% of AUC and 84.67% of accuracy on 5-shot learning. Likewise, the proposed model achieved 83.34% of AUC and 84.61% of accuracy on 3-shot learning and also the same model achieved 89.60% of AUC and 91.28% of accuracy on 5-shot learning. From this experiment analysis, it is clearly shows that the proposed model achieved better performance to classify the unseen skin cancer diseases.

5. Conclusion

Skin cancer picture classification was formulated as a few-shot learning issue for our relation-embedding network, which relies on meta-learning. Using the ISIC 2018 dataset for meta training and the SD-198 dataset for meta testing, we are able to identify two separate skin lesions. Two modules are used for skin cancer identification, six different classes are used for meta training and two classes such as lentigo melanoma and acral melanoma are used for meta testing. Unknown classes are discovered using the embedding metric mapping module when the support set image and query image are paired in the few-shot learning pattern. The location detection module uses YoloV5 network uses the boundary boxes to identify the location of lesions in query image by annotating the SD-198 dataset images. The feature vector is extracted by max norm CNN model, where the module of embedding metric mapping is used to identify the cosine similarity and cosine distance between feature vectors. By using the 5-shot learning process, the average accuracy of proposed model is 85.70% and 83.10% of accuracy on ISIC-2018 dataset, where existing technique achieved 79.01% of average accuracy and 80.19% of accuracy on the same dataset. In the future work, the different classes of skin cancer are considered for unseen query set.

References

- [1] Apalla Z, Nashan D, Weller RB, Castellsagué X. Skin Cancer: Epidemiology, Disease Burden, Pathophysiology, Diagnosis, and Therapeutic Approaches. *Dermatol Ther (Heidelb)* 2017;7:5–19. <https://doi.org/10.1007/s13555-016-0165-y>.
- [2] Zakhem GA, Fakhoury JW, Motosko CC, Ho RS. Characterizing the role of dermatologists in developing artificial intelligence for assessment of skin cancer: A systematic review. *J Am Acad Dermatol* 2020. <https://doi.org/10.1016/j.jaad.2020.01.028>.
- [3] Saba T. Recent advancement in cancer detection using machine learning: Systematic survey of decades, comparisons and challenges. *J Infect Public Health* 2020;13:1274– 89. <https://doi.org/10.1016/j.jiph.2020.06.033>.
- [4] Didona D, Paolino G, Bottoni U, Cantisani C. Non melanoma skin cancer pathogenesis overview. *Biomedicines* 2018;6:1–15. <https://doi.org/10.3390/biomedicines6010006>.
- [5] Naresh Kumar S, Mohammed Ismail B. Systematic investigation on Multi-Class skin cancer categorization using machine learning approach. *Mater Today Proc* 2020. <https://doi.org/10.1016/j.matpr.2020.11.484>.
- [6] Ciążyńska M, Kamińska-Winciorek G, Lange D, Lewandowski B, Reich A, Sławińska M, et al. The incidence and clinical analysis of non-melanoma skin cancer. *Sci Rep* 2021;11:1–10. <https://doi.org/10.1038/s41598-021-83502-8>.

- [7] Filippi L, Bruno G, Domazetovic V, Favre C, Calvani M. Current therapies and new targets to fight melanoma: A promising role for the β 3-adrenoreceptor. *Cancers (Basel)* 2020;12:1–16. <https://doi.org/10.3390/cancers12061415>.
- [8] WHO. Radiation: Ultraviolet (UV) radiation and skin cancer 2017. [https://www.who.int/news-room/q-a-detail/radiation-ultraviolet-\(uv\)-radiation-and-skin-cancer](https://www.who.int/news-room/q-a-detail/radiation-ultraviolet-(uv)-radiation-and-skin-cancer) (accessed March 17, 2021).
- [9] Setiawan AW. Effect of Color Enhancement on Early Detection of Skin Cancer using Convolutional Neural Network. 2020 IEEE Int Conf Informatics, IoT, Enabling Technol ICIoT 2020 2020:100–3. <https://doi.org/10.1109/ICIoT48696.2020.9089631>.
- [10]. Mitchell, T.M. *Machine Learning*; OCLC 36417892; McGraw Hill: New York, NY, USA, 1997; pp. 1–432.
- [11] Colin Raffel, Noam Shazeer, Adam Roberts, Katherine Lee, Sharan Narang, Michael Matena, Yanqi Zhou, Wei Li, and Peter J. Liu. Exploring the limits of transfer learning with a unified text-to-text transformer, 2019.
- [12] Taibou Birgui Sekou, Moncef Hidane, Julien Olivier, and Hubert Cardot. From patch to image segmentation using fully convolutional networks - application to retinal images. *ArXiv*, abs/1904.03892, 2019.
- [13] Oriol Vinyals, Charles Blundell, Timothy Lillicrap, Koray Kavukcuoglu, and Daan Wierstra. Matching networks for one shot learning. In *Proceedings of the 30th International Conference on Neural Information Processing Systems, NIPS'16*, page 3637–3645, Red Hook, NY, USA, 2016. Curran Associates Inc.
- [14] Jake Snell, Kevin Swersky, and Richard Zemel. Prototypical networks for few-shot learning. In *Advances in neural information processing systems*, pages 4077–4087, 2017.
- [15] Joaquin Vanschoren. Meta-learning: A survey. *CoRR*, abs/1810.03548, 2018.
- [16] Risto Vuorio, Shao-Hua Sun, Hexiang Hu, and Joseph J. Lim. Multimodal model-agnostic meta-learning via taskaware modulation. In *Neural Information Processing Systems*, 2019.
- [17] Viraj Prabhu, Anitha Kannan, Murali Ravuri, Manish Chaplain, David Sontag, and Xavier Amatriain. Few-shot learning for dermatological disease diagnosis. In *Finale Doshi-Velez, Jim Fackler, Ken Jung, David Kale, Rajesh Ranganath, Byron Wallace, and Jenna Wiens, editors, Proceedings of the 4th Machine Learning for Healthcare Conference*, volume

106 of Proceedings of Machine Learning Research, pages 532–552, Ann Arbor, Michigan, 09–10 Aug 2019. PMLR.

[18] Li, X., Yu, L., Jin, Y., Fu, C.W., Xing, L. and Heng, P.A., 2020, October. Difficulty-aware meta-learning for rare disease diagnosis. In International Conference on Medical Image Computing and Computer-Assisted Intervention (pp. 357-366). Springer, Cham.

[19]. Filali, Y.; Khoukhi, H.; Sabri, M.A.; Aarab, A. Efficient fusion of handcrafted and pre-trained CNNs features to classify melanoma skin cancer. *Multimed. Tools Appl.* 2020, 79, 31219–31238.

[20]. Amin, J.; Sharif, A.; Gul, N.; Anjum, M.; Nisar, M.; Azam, F.; Bukhari, S. Integrated design of deep features fusion for localization and classification of skin cancer. *Pattern Recognit. Lett.* 2020, 131, 63–70.

[21]. Bajwa, M.; Muta, K.; Malik, M.; Siddiqui, S.; Braun, S.; Homey, B.; Dengel, A.; Ahmed, S. Computer-Aided Diagnosis of Skin Diseases Using Deep Neural Networks. *Appl. Sci.* 2020, 10, 2488.

[22]. Bi, L.; Feng, D.; Fulham, M.; Kim, J. Multi-Label classification of multi-modality skin lesion via hyper-connected convolutional neural network. *Pattern Recognit.* 2020, 107, 107502.

[23] Z. Xu, F. R. Sheykhahmad, N. Ghadimi, and N. Razmjooy, “Computer-aided diagnosis of skin cancer based on soft computing techniques,” *Open Medicine*, vol. 15, no. 1, pp. 860–871, 2020.

[24] N. Dey, V. Rajinikanth, H. Lin, and F. Shi, “A study on the bat algorithm technique to evaluate the skin melanoma images,” in *Applications of Bat Algorithm and its Variants*, pp.

45–60, Springer, Singapore, 2021.

[25] Noel Codella, Veronica Rotemberg, Philipp Tschandl, M Emre Celebi, Stephen Dusza, David Gutman, Brian Helba, Aadi Kallou, Konstantinos Liopyris, Michael Marchetti, et al. Skin lesion analysis toward melanoma detection 2018: A challenge hosted by the international skin imaging collaboration (isic). arXiv preprint arXiv:1902.03368, 2019.

[26] Xiaoxiao Sun, Jufeng Yang, Ming Sun, and Kai Wang. A benchmark for automatic visual classification of clinical skin disease images. In *European Conference on Computer Vision*, pages 206–222. Springer, 2016.

[27] Yan, B., Fan, P., Lei, X., Liu, Z. and Yang, F., 2021. A real-time apple targets detection method for picking robot based on improved YOLOv5. *Remote Sensing*, 13(9), p.1619.

[28] Mahajan, K., Sharma, M. and Vig, L., 2020. Meta-dermdiagnosis: Few-shot skin disease identification using meta-learning. In Proceedings of the IEEE/CVF Conference on Computer Vision and Pattern Recognition Workshops (pp. 730-731).

[29] Singh, R., Bharti, V., Purohit, V., Kumar, A., Singh, A.K. and Singh, S.K., 2021. MetaMed: Few-shot medical image classification using gradient-based meta-learning. Pattern Recognition, 120, p.108111.